PEO Temporary Network in PEO/PMMA Blends: NMR Approach

A. Guillermo,* C. Lartigue, and J. P. Cohen Addad

Laboratoire de Spectrométrie Physique, associé au CNRS (UMR C5588), Université J. Fourier Grenoble I, B.P. 87, 38402, Saint Martin d'Hères Cedex, France

Received June 10, 1997; Revised Manuscript Received October 14, 1997[⊗]

ABSTRACT: Transverse magnetic relaxation properties of protons attached to PEO chains were investigated in compatible blends of hydrogenated PEO and deuterated PMMA by varying the PEO concentration and the temperature. The onset of segmental fluctuations is observed for samples that do not crystallize ($\phi \leq 0.31$); it occurs above T_g(PEO) but below the blend glass transition temperature, $T_g(\phi)$. At higher temperatures, for all concentrations, relaxation curves exhibit a solid-like behavior typical of a residual dipolar interaction due to the presence of a temporary network. The associated relaxation time obeys a linear temperature dependence with a reference at $T_g(\phi) + T_0$ and a linear variation with the mean segmental spacing between two consecutive entanglements along PEO chains, as calculated from the model proposed by Tsenoglou. This study extends the relationship between NMR properties and the network mesh size already observed in permanent gels and entangled homopolymers to miscible heteropolymers.

1. Introduction

The concept of entanglement is currently used to analyze the property of temporary elasticity in polymers.[1] How can it be applied to polymer blends? In miscible blends, each species brings to the blend a separate dynamic behavior governed by its own intrinsic properties, mainly the monomeric friction factor and the molecular weight between entanglements. The changes that occur in the local environment of each blend component may modify their fractional free volume and thermal expansion coefficient, as well as the glass transition temperature, which is concentration dependent. In various compatible blends, a single but broad glass transition is observed; it is often analyzed in terms of dynamic microheterogeneities;[2−4] the role played by local concentration fluctuations and/or by differences in the monomeric friction coefficients has been addressed.[4,5] Complex temperature and concentration dependences of the individual local dynamic properties have been shown:[4−14] the thermal behavior has been described using an effective glass transition temperature for each species, $T_g^*(\phi)$, instead of the DSC glass transition temperature of the blend;[4,6−8] a failure of the time-temperature equivalence of the viscoelastic properties has been reported.[5,6,8−10] At a large spatial scale, because there is no direct measurement of the entanglement mesh size, the blending effect on the temporary network in blends remains an open question. Is there a single network or is there a network for each component, and how is it influenced by the presence of the second component? The amplitude of the dynamic modulus of each blend component has been estimated from rheological measurements combined with birefringence and IR dichroism for blends of 1,4-polyisoprene and 1,2-polybutadiene; from these values, the entanglement spacing per chain, the tube diameter, and the monomeric friction coefficients, $\zeta_{0,i}$, calculated for each species within the framework of the reptation model have been shown to be concentration dependent.[5,6] In this particular blend, a similar concentration dependence of the entanglement molecular weight has been found for both components (which does not allow a precise determination of the effect of blending on the entanglements), while strong temperature and concentration variations have been shown for $\zeta_{0,i}$, the high-T_g component (1,2-PB) being more sensitive to the addition of 1,4PI and also more sensitive to increasing temperature. Here, we have attempted to determine the concentration dependence of the entanglement spacing in PEO/PMMA blends by using proton NMR and selective deuterium labeling of one component.

NMR is a suitable tool for investigating both the chain segmental fluctuations and the statistical structure of permanent or temporary polymer networks. On the one hand, fast random motions are characterized from the longitudinal relaxation of the magnetization. On the other hand, the transverse magnetic relaxation is sensitive to long range constraints distributed along a polymer chain, which may be pictured as being due to interchain coupling junctions. They create an anisotropy of the random local motions along chain segments, giving rise to solid-like NMR properties that are related to the mean segmental spacing between entanglements or cross-links.[15−18]

Using proton magnetic relaxation, we investigated the dynamics of hydrogenated PEO chains embedded in a matrix of deuterated PMMA chains for a series of entangled PEO/PMMA blends with various compositions. Among binary blends, one peculiarity of the PEO/PMMA system lies in the large difference between the glass transition temperature of the two components, almost 200 K. Miscibility of PEO and PMMA has been demonstrated.[9,19,20] Small values of the interaction parameter χ were reported,[20−24] indicating only weak interactions. In a previous study, we investigated the properties of local random motions of PEO chain segments obtained from the analysis of the spin−lattice relaxation rate.[19] In this work, we report on the properties of the transverse magnetic relaxation of protons attached to PEO chains. First, we characterize the nature of the relaxation curve as a function of concentration through its thermal behavior. The existence of a residual dipolar interaction due to that of a

[⊗] Abstract published in *Advance ACS Abstracts,* December 15, 1997.

S0024-9297(97)00836-X CCC: $15.00
Published on Web 01/15/1998

temporary network is shown from the so-called pseudosolid properties of the transverse relaxation. Secondly, we attempt to perform a quantitative characterization of the PEO network in the blends as a function of concentration from the temperature dependence of the relaxation rate associated to the residual interaction. Results are compared to those obtained for entangled polybutadiene (PB) chains[25] and for calibrated networks of poly(propylene oxide) (PPG) chains.[15] The discussion is based on the concentration dependence of the mean spacing between PEO entanglements calculated from the properties of each blend component using the model proposed by Tsenoglou.[26]

2. Experimental Section

Sample Preparation and Characterization. Hydrogenated PEO-h (M_w = 150 000, I_p = 1.07) and deuterated PMMA-d (M_w = 262 000, I_p = 1.08, deuteration ≥ 99%) components were both obtained from Polymer Laboratories. The PMMA tacticity was determined by high-resolution NMR: it contains 9 ± 2% isotactic, 45 ± 5% heterotactic, and 46 ± 5% syndiotactic triads. Blends were prepared from 1% benzene solutions maintained for 2−3 days at 40 °C. Progressive evaporation of the solvent was carefully monitored over 1 day by raising the temperature slowly to 75 °C, i.e., slightly above the PEO melting point, $T_m \approx 343$ K.[23] Subsequent annealing was done under vacuum at 120 °C for 2 h in order to remove any traces of solvent. Blends with a PEO volume fraction ϕ of 20%, 31%, 41%, 51%, and 71% as well as pure PEO samples were prepared in the same way.

Miscibility of the two components was checked from measurements of the glass transition temperature using differential scanning calorimetry (DSC) and from measurements of the proton spin−lattice relaxation time T_1 using NMR. The observation of a single T_g or T_1 and their concentration dependence guarantee that no large-scale heterogeneities occur in the samples. The glass transition temperature was found to obey a Fox equation, $1/T_g(w) = w/T_g(\text{PEO}) + (1 - w)/T_g(\text{PMMA})$, with $T_g(\text{PEO}) = 221 \pm 5$ K and $T_g(\text{PMMA}) = 399 \pm 5$ K, w being the PEO weight fraction.[19]

Crystallization of PEO takes place at temperatures close to the PEO melting point but only for PEO volume fractions higher than 31%; at lower concentrations, samples remain amorphous.

Further details regarding the preparation and the characterization of samples may be found in ref 19.

NMR Measurements. NMR experiments were performed at 60 MHz using a Bruker MSL100 spectrometer. Transverse magnetic relaxation curves were determined by using a modified Carr−Purcell spin-echo sequence including the phase cycling ($x, -x, -x, x$) of the $(180°)_x$ pulses; at low temperatures, relaxation curves were directly obtained from the free induction decay (FID) following the $(90°)_x$ rotation pulse. Pseudosolid spin echoes were recorded using the following pulse sequence:[27]

$$(90°)_x-[\tau-(180°)_x-2\tau-(180°)_{-x}-2\tau-(180°)_{-x}-2\tau-(180°)_x-\tau]-(90°)_y-[\tau_1-(180°)_x-2\tau_1-(180°)_{-x}-2\tau_1-(180°)_{-x}-2\tau_1-(180°)_x-\tau_1]_n$$

Relaxation curves of protons attached to PEO chains in PMMA-d/PEO-h blends were measured as a function of temperature and PEO concentration. All samples were kept in glass tubes sealed under vacuum; the sample temperature was controlled to within ±1 K. The temperature was varied from 170 to 430 K; at higher temperatures, there is a risk of sample degradation.

3. NMR Approach

The NMR investigation of the statistical structure of molten polymeric systems at a semilocal space scale involves a two-step motional averaging process of the anisotropic spin interactions. The method has been described in detail elsewhere[16] and is briefly summarized here. We consider only dipole−dipole interactions between protons that belong to a given chain segment. The static dipole−dipole interaction observed in the solid state becomes time-dependent with increasing temperature due to the progressive onset of fast isomerization processes. It leads to an averaging of the interaction over configurational changes known as the motional narrowing process and which may occur in two steps for polymers. Indeed, for entangled or cross-linked chains, even at temperatures well above the glass transition temperature, this averaging process is not complete owing to a slight anisotropy of random rotations of monomeric units that belong to chain segments defined by coupling junctions, such as entanglements or cross-links. It yields a residual dipolar interaction and a so-called pseudosolid behavior of the corresponding transverse relaxation of the nuclear magnetization. Its existence can be revealed using various specific NMR experiments;[16,28,29] in this work, it will be detected from the presence of pseudosolid echoes.

For polymer networks, whether they are permanent or temporary, the characteristic relaxation time τ of the transverse magnetic relaxation, when governed by the residual dipolar interaction, has been shown to obey a linear dependence on both the temperature and the mean segmental spacing between cross-links or entanglements. For calibrated gels of end-linked poly(propylene oxide) chains, the following equation has been established:[15]

$$\tau = [\gamma_s M_n + s_0][T - T_g(M_n) - T_0] \qquad (1)$$

where τ is the inverse of the so-called NMR structural parameter χ_c,[16] M_n is the molecular weight of the polymer precursor, and $T_g(M_n)$ is the glass transition temperature of the gel, a decreasing function of its mesh size; γ_s, s_0, and T_0, are numerical constants.

A similar relationship has been found for the relaxation time of protons attached to entangled polybutadiene chains in a melt or in concentrated solutions:[25]

$$\tau = A\left[1 + \frac{B}{G_N^0(x,\phi)}\right][T - T_g(x,\phi) - T_0] \qquad (2)$$

where x is the 1,2 vinyl content, which controls the polymer microstructure, ϕ is the polymer volume fraction, and $G_N^0(x,\phi)$ is the viscoelastic plateau modulus; A, B, and T_0, are numerical constants. $G_N^0(x,\phi)$ is inversely proportional to $M_e(x,\phi)$, the average molecular weight between entanglements of the polymer in solution; it has been found to be equal to $G_N^0\phi^{2.2}$, which shows the widening of the polybutadiene entanglement network upon dilution.

In both cases, PPG networks and entangled PB chains, the glass transition temperature of the system appears as a reference temperature of the thermal behavior of the magnetic relaxation time, but with a temperature shift T_0 that is slightly dependent on the system, 42 and 50 K, respectively. On the other hand, the slope of this linear thermal dependence varies linearly with the mesh size of the statistical structure defined by interchain coupling junctions. It must be noted that such a correlation between NMR properties and the statistical structure of polymer network has also

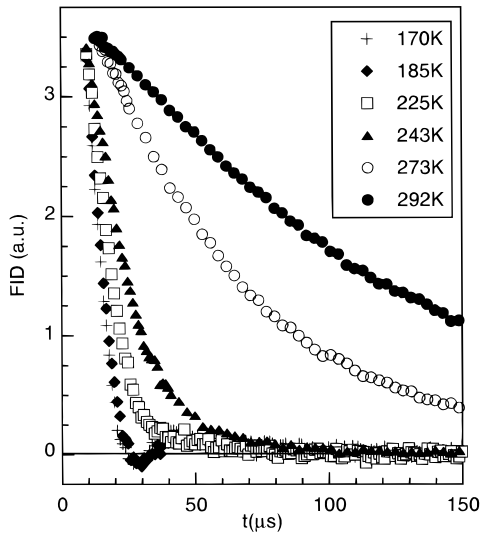

Figure 1. Thermal evolution of the transverse magnetic relaxation (in-phase component of the FID) of protons attached to PEO chains in the PEO/PMMA blend with $\phi = 0.20$.

been demonstrated using transverse ^{2}H quadrupolar relaxation,[18] or ^{1}H−^{13}C couplings.[17,30]

In the case of long polymer chains in a melt or in concentrated solutions, a temporary network structure is perceived because the interchain coupling junctions dissociate sufficiently slowly so that they can be pictured as temporarily fixed points. But, for lower molecular weight or dilute solutions, and with increasing temperature, fluctuations of orientation of the coupling junctions may become fast enough to yield a complete averaging of the dipolar interaction.[31,32] This process is the second step of the motional narrowing.[16] At this stage, the transverse magnetic relaxation has a liquid-like behavior; it may be used to characterize the whole chain dynamics.[31−33]

4. Characterization of the Relaxation Function

From the noncrystalline samples, i.e., at a PEO volume fraction $\phi \leq 0.31$, we will show the progressive effect of the motional averaging of dipole−dipole interactions when the temperature is raised starting from below T_g(PEO). Then, for all concentrations and above the PEO melting point, we will examine the temperature dependence of the properties of the relaxation curves.

4.1. Thermal Behavior: Partial Motional Averaging. For low PEO concentration blends that do not crystallize, the thermal behavior of the relaxation curve was investigated from 170 up to 430 K, i.e., from well below T_g(PEO) up to well above T_g(blend). For $\phi = 0.20$, at 170 and 185 K, the decay of the relaxation is very rapid, as shown in Figure 1: the transverse magnetization presents a damped oscillation with a minimum at 30 μs. Such a rapid relaxation is typical of a solid state. For comparison, we have calculated the relaxation function for one single pair of protons imbedded in a solid matrix:[34] it is characterized by a first minimum that occurs at 35 μs when the distance between the two spins is set equal to the interproton distance in a CH_2 group (1.78 Å).

With increasing temperature, the duration of the decay increases continuously and the shape of the curve is qualitatively modified. A pseudosolid behavior is detected from the presence of pseudosolid echoes at any temperature up to 430 K; an example is given in Figure 2 at 343 K $\approx T_g(\phi = 0.20)$. It indicates that the relaxation mechanism is dominated by the residual dipolar spin−spin interaction of protons. The transition from the solid to a pseudosolid behavior results from the increased rate of the segmental fluctuations.

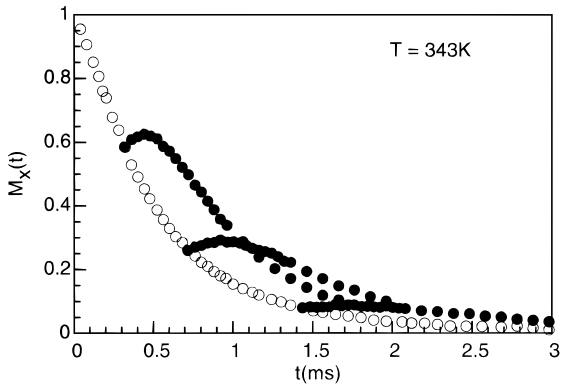

Figure 2. Pseudo-solid spin echoes recorded at 343K in the PEO/PMMA blend with $\phi = 0.20$; (○): normalized relaxation function; (●) echoes formed at 0.32, 0.72, and 1.44 ms.

The same properties of the relaxation function were found for $\phi = 0.31$, with the rigid state of PEO chains again observed below T_g(PEO).

There are two striking features of the thermal dependence of these NMR relaxation curves: firstly, the solid state of PEO chains in PEO/PMMA blends (observable only at low PEO concentration) is perceived below T_g(PEO); secondly, the first step of the motional averaging takes place below the glass transition temperature of the blend. This is in qualitative agreement with our previous study of the properties of the spin−lattice relaxation rate of protons in the same blends: the thermal behavior of the local PEO dynamics was already found to be related to T_g(PEO) at any concentration, while molecular motion rates were found to be strongly influenced by the presence of PMMA chains.[19]

At higher PEO concentrations, $\phi > 0.40$, measurements were performed only on molten blends (i.e., above the PEO melting temperature). For these blends, pseudosolid echoes were also observed at any temperature in the range 343 K $\leq T \leq$ 430 K.

4.2. Property of Time−Temperature Superposition: Concentration Dependence. The effect of diluting PEO chains in a matrix of PMMA shortens the time scale of the relaxation of protons attached to PEO chains at a given temperature. An example is shown in the pseudosolid regime, at 343 K, in Figure 3: a reduction factor of 5 in time is observed for the blend containing 20% PEO compared to the homopolymer PEO. When the temperature is raised, the difference becomes less pronounced. However, the shape of the relaxation curves measured as a function of PEO concentration is qualitatively different at any temperature within the range of observation ($T <$ 430 K).

For $\phi = 0.20$, the shape of relaxation functions is found to be invariant over a large temperature range starting at 274 K, as shown in Figure 4a: the complete relaxation curves are superimposed on each other by applying suitable factors to the time scale of measurements. The property of superposition shows that the nature of the mechanism of magnetic relaxation does not change in the temperature range of observation (150 degrees at this concentration). The shift factor increases rapidly, which accounts for the change of the time scale

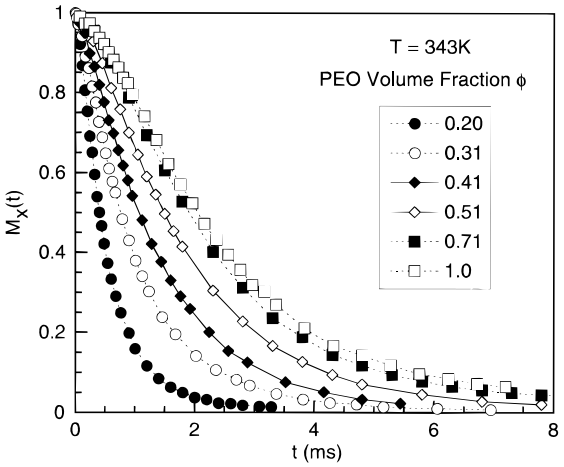

Figure 3. Transverse magnetic relaxation of protons attached to PEO chains in PEO/PMMA blends as a function of the PEO volume fraction (T = 343 K).

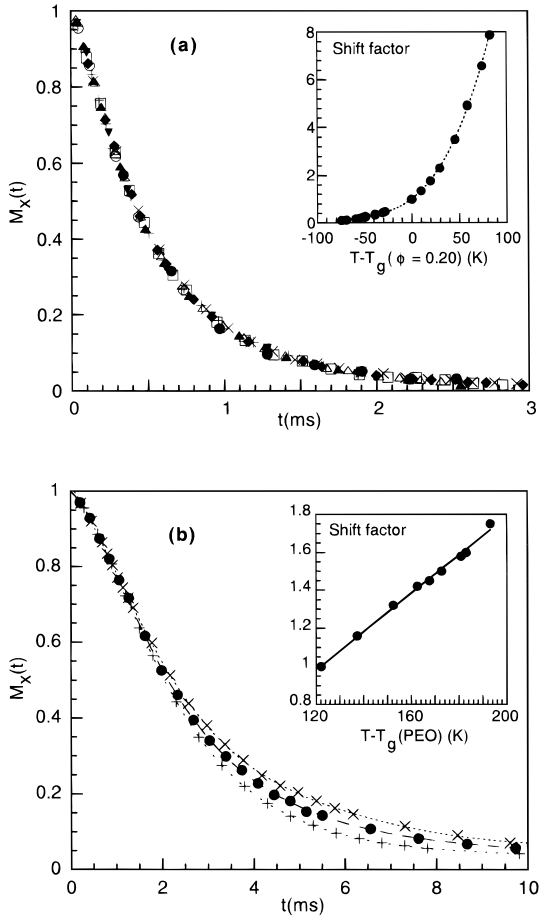

Figure 4. Time−temperature superposition (see text) at reference temperature T_0 = 343 K: (a) ϕ = 0.20 [(●) 274 K; (×) 294 K; (□) 313 K; (◆) 343 K; (△) 363 K; (+) 389 K; (▲) 402 K; (○) 417 K; (▼) 426 K]; (b) ϕ = 1.0 [(+) 343 K; (●) 384 K; (×) 414 K]. Each insert displays the temperature dependence of the shift factor.

of the relaxation with increasing temperature (see insert Figure 4a). For ϕ = 0.31, the shape of relaxation curves was also found to be invariant from T = 274 K. This is the temperature at which the pseudosolid behavior of the relaxation is established and it is equal to T_g(PEO) + 50 K, a typical value already observed for several homopolymers.[16] With increasing PEO concentration, the property of invariance no longer holds along the

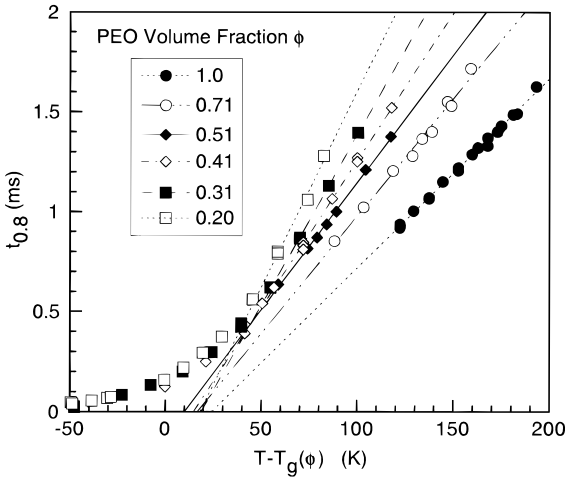

Figure 5. Temperature dependence of the time interval $t_{0.8}$-(ϕ) corresponding to 80% of the amplitude of the relaxation curves as a function of the PEO volume fraction. Lines are linear fits to the data for $T - T_g(\phi) \geq 50$ K.

whole relaxation function: the part of the relaxation curves that is superposed decreases progressively. The observed change of shape of the relaxation curve with increasing temperature reveals a change in the nature of the mechanism of relaxation. For ϕ = 1.0 and 343 K < T < 430 K, a good superposition is obtained for $M_x(t) \geq 0.75$, as shown in Figure 4b; the shift factor varies linearly with temperature (see insert Figure 4b). At lower amplitudes, the relaxation curve is slightly lengthened toward longer times.

This latter behavior is typical for entangled polymer melts: heating leads to an increase of the fluctuation rate of the coupling junctions, which is first detected in the long time part of the relaxation curve. It illustrates the progressive onset of the second step of the motional averaging process. However, the lengthening observed in the pure PEO relaxation curves between the two extreme temperatures is small compared to the applied shift factor (see Figure 4b) and pseudosolid echoes are still observed at any temperature: it implies that relaxation functions remain mainly governed, at any temperature, by the residual dipolar interaction. At low PEO concentration, the invariance of the shape of the relaxation curves in the observed temperature range indicates that the fluctuation rate of the coupling junctions becomes too slow to be detected. In the following, we will concentrate our analysis on the upper part of the relaxation curves where fluctuations of the intercoupling junctions vector are not experimentally detected: this part is representative of the statistical structure of the temporary network at any concentration.

5. Discussion: Concentration Dependence of the PEO Network in PEO/PMMA Blends

Following the above conclusions, we investigated the concentration dependence of the PEO temporary network structure through the temperature dependence of the characteristic time $t_{0.8}$, the time required for the transverse magnetization to decay to 80% of its initial value. Its variation is plotted as a function of $T - T_g$-(ϕ) in Figure 5. A linear dependence is found in the range restricted to $T - T_g(\phi) \geq 50$ K; lines are extrapolated to zero when the temperature interval $T - T_g(\phi)$ is equal to T_0 where $T_0 = 17 \pm 5$ K independent of the

concentration. This leads to the expression

$$t_{0.8}(T,\phi) = s(\phi)\,[T - T_g(\phi) - T_0] \tag{3}$$

The reference temperature defined by $T_g(\phi) + T_0$ is strongly concentration dependent due to $T_g(\phi)$. The temperature dependence expressed in eq 3 is similar to that of PPG (eq 1) and PB networks (eq 2), in which $s(\phi)$ has been shown to vary linearly with M_n and $M_e(x,\phi)$ respectively. To proceed further with the comparison of PEO/PMMA blends and PPG or PB networks, an estimation of the average molecular weight between entanglements along PEO chains is required.

Tsenoglou has proposed a model to predict the composition dependence of entanglements for miscible heteropolymer blends,[26] which we briefly summarize. The model assumes complete randomness in the formation of entanglements. In the pure state, each chain i is characterized by its molecular weight M_i, its density ρ_i and its molecular weight between entanglements M_{ei0}. In the blend, let N_{ij} be the number of segments along a chain of type i which are determined by entanglements of this chain with two chains of type j ($N_{ij} \gg 1$) and M_{eij} the average molecular weight of such segments. The total number of entanglements per chain i is given by the sum over entanglements with all species in the blend:

$$N_i = \sum_{j=1}^{m} N_{ij} \approx \sum_{j=1}^{m} \frac{M_i}{M_{eij}} \tag{4}$$

The entanglement probability between two different species is shown to be proportional to the geometric average of the entanglement probabilities between similar chains. On this basis, the molecular weight between two successive entanglements of the same polymer j along a chain i can be evaluated:

$$M_{eij} = \frac{1}{\phi_j}\left(\frac{M_{ei0}M_{ej0}}{\rho_j / \rho_i}\right)^{1/2} \tag{5}$$

where ϕ_j is the volume fraction of the jth component. Finally, in a binary blend, the mean molecular weight between entanglements along a chain i of volume fraction ϕ_i in the blend is

$$\frac{M_{ei0}}{M_{ei}(\phi_i)} = \phi_i\left(1 + \frac{1-\phi_i}{\phi_i}\,k\right) \tag{6}$$

with $k = (\rho_j M_{ei0} / \rho_i M_{ej0})^{1/2}$. This model yields separate entanglement molecular weights for each blend component, M_{e1} and M_{e2}, both of which depend on the blend composition.

However, eq 6 does not account for specific interactions between dissimilar species, which may modify the probability of entangling in blends. Tsenoglou has developed an extended theory by adding two parameters: ϵ_{ij}, which represents the relative strength of these interactions, and n, which is set to $+1$ or -1 depending on their attractive or repulsive character. In the case of a binary blend, ϵ_{12} and ϵ_{21} are set equal to a single value ϵ and eq 6 now becomes

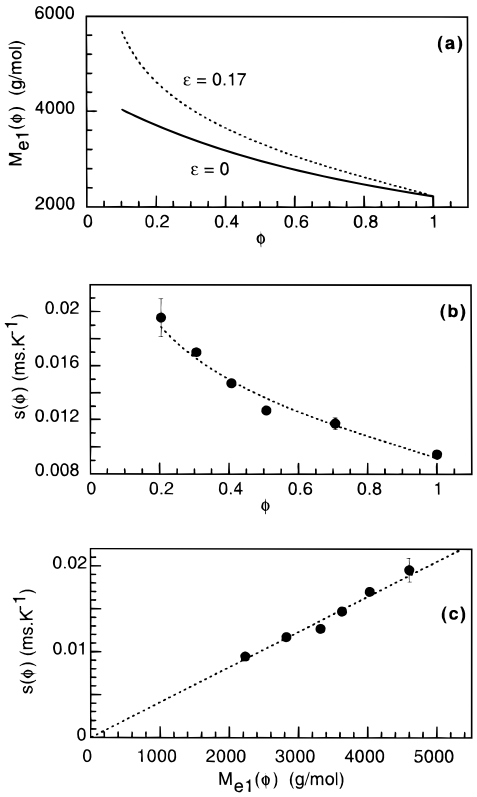

Figure 6. (a) Molecular weight between entanglements $M_{e1}(\phi)$ for PEO in PEO/PMMA blends calculated from the model of Tsenoglou (eq 7): (continuous line) $\epsilon = 0$; (dotted line) $\epsilon = 0.17$. (b) PEO volume fraction dependence of the slope of lines drawn in Figure 5, $s(\phi)$. (c) $s(\phi)$ versus $M_{e1}(\phi)$ calculated for $\epsilon = 0.17$. The dotted line in (b) and (c) is the best fit of eq 8 with $s_0 = 0$ and $M_{e1}(\phi)$ calculated from eq 7 with $\epsilon = 0.17$ and $n = -1$.

$$\frac{M_{ei0}}{M_{ei}(\phi_i)} = \phi_i\left(1 + \epsilon\frac{1-\phi_i}{\phi_i}\,k\right)^n + (1-\phi_i)k\left[\left(1 + \epsilon\frac{1-\phi_i}{\phi_i}\,k\right)\left(1 + \epsilon\frac{\phi_i}{1-\phi_i}\,\frac{1}{k}\right)\right]^{n/2} \tag{7}$$

which reduces to eq 6 for the special case of ϵ and n equal to zero.

For PEO/PMMA blends, Tsenoglou estimated ϵ and n using the concentration dependence of the viscoelastic plateau modulus measured by Wu[35] and he obtained $\epsilon = 0.17$ and $n = -1$. The PEO network mesh size, $M_{e1}(\phi)$, is then easily calculated from eq 7 where the subscripts 1 and 2 refer to PEO and PMMA, respectively, and where we have taken the following values also from Wu:[35] $\rho_1 = 1.064$ g·cm^{-3}, $\rho_2 = 1.095$ g·cm^{-3}, $M_{e10} = 2230$ g/mol, and $M_{e20} = 9130$ g/mol. Its concentration dependence is plotted in Figure 6a for the two cases, $\epsilon = 0$ and $\epsilon = 0.17$. In the range of concentration investigated, $M_{e1}(\phi)$ increases from 2230 for PEO to 3700 at $\phi = 0.20$ with $\epsilon = 0$, but to 4600 with $\epsilon = 0.17$; that is a difference of 25% in $M_{e1}(\phi)$ at $\phi = 0.20$. It shows the effect of the polymer−polymer interactions as taken into account via ϵ and n: the PEO network mesh size increases faster with increasing PMMA content. More generally, the analysis of Tsenoglou shows that the statistical structure of each component network in blends is influenced by the polymer−polymer interactions, even when they are weak, as is the case

for PEO/PMMA blends. In the following, we use the concentration dependence of the PEO entanglement spacing in the blends PEO/PMMA calculated with eq 7 and $\epsilon = 0.17$.

The concentration dependence of the slope $s(\phi)$ characterizing the linear thermal behavior of the relaxation time $t_{0.8}(T,\phi)$ for PEO (eq 3) is shown in Figure 6b. Following the results for PPG (eq 1) and PB networks (eq 2), we analyze $s(\phi)$ according to the linear equation

$$s(\phi) = \gamma M_{e1}(\phi) + s_0 \tag{8}$$

where values of $M_{e1}(\phi)$ are calculated as above. In Figure 6c, $s(\phi)$ is plotted versus $M_{e1}(\phi)$: it is found to be directly proportional to $M_{e1}(\phi)$. The temperature and concentration dependence of the NMR relaxation time is then

$$t_{0.8}(T,\phi) = \gamma M_{e1}(\phi)[T - T_g(\phi) - T_0] \tag{9}$$

where $\gamma = 4.11(3) \times 10^{-6}$ ms·K^{-1} (g/mol)$^{-1}$.

The main point here is the analogy established with PPG networks and entangled polymers: the conclusions of refs 15 and 25 for homopolymer systems are extended to one component of a compatible binary polymer blend. At first, the transverse magnetic relaxation is directly related to the chain segment length between interchain junctions (eqs 1, 2, and 9). Secondly, the temperature factor that controls the thermal behavior of the relaxation rate is referred to the glass transition temperature of the polymer system; it is supposed to be related to the chain stiffness on which depends the residual dipole−dipole interaction determined by the degree of anisotropy of random rotations of monomeric units.[16]

For PEO in PEO/PMMA blends, the relationship between the NMR relaxation time and the network mesh size (eq 9) could only be obtained by using a predictive model for the composition dependence of the entanglement spacing. We have used the model of Tsenoglou, which predicts separate entanglement molecular weights for each blend component (eq 7). Within experimental error, we demonstrate that the predictions of Tsenoglou are consistent with the analysis of NMR properties of PEO. A further check of the validity of the model for PEO/PMMA blends would require a similar study of the NMR properties of the PMMA component. Finally, it is noteworthy that for blends of 1,4-polyisoprene and 1,2-polybutadiene, the analysis of the amplitude of the viscoelastic modulus measured for each blend component shows that each component has a different mean entanglement spacing, which is found in agreement with the predictions of Tsenoglou.[6]

6. Conclusion

In this work, we investigate the properties of the transverse magnetic relaxation of protons attached to PEO chains in a series of entangled hydrogenated-PEO/deuterated-PMMA blends with varying composition and temperature.

For low PEO concentration samples that do not crystallize ($\phi = 0.20$ and 0.31), the solid state of the polymer is observed from the shape of the relaxation curve: it occurs at temperatures lower than the glass transition temperature of PEO itself, T_g(PEO) ≈ 221 K. With increasing temperature, the onset of the fast isomerization process is perceived already at temperatures well below the glass transition temperature of the blends.

The existence of a temporary entanglement network is detected from the pseudosolid behavior of the magnetization relaxation due to a local anisotropy of the rotational isomerizations. Above the glass transition temperature of the blend, which increases with decreasing PEO concentration, the transverse relaxation time associated with the PEO temporary network follows the same thermal dependence, whatever the blend composition: it increases linearly with the temperature interval $(T - T_g(\phi) - T_0)$, where T_0 is independent of the blend composition. This behavior resembles that which characterizes a network structure, as was demonstrated for calibrated end-linked poly(propylene oxide) chains[15] and entangled polybutadiene melts.[25] But it reflects only one aspect of this characteristic behavior. The second aspect is a direct dependence of the relaxation time with the mean segmental spacing between cross-links or entanglements. For the PEO/PMMA binary polymer blend, we calculate this latter parameter from the predictions of Tsenoglou. The NMR relaxation time is shown to follow the concentration dependence predicted by Tsenoglou for the network mesh size of one blend component in miscible heteropolymer blends.

This work contributes to extend the relationship that exists between NMR and network properties for homopolymer systems to compatible binary polymer blends. It supports the Tsenoglou entanglement theory that predicts individual entanglement spacings for each species.

References and Notes

(1) Ferry, J. D. *Viscoelastic Properties of Polymers*, 3rd ed.; Wiley: New York, 1980.
(2) Schmidt-Rohr, K.; Clauss, J.; Spiess, H. W. *Macromolecules* **1992**, *25*, 3273.
(3) Chin, Y. H.; Zhang, C.; Wang, P.; Inglefield, P. T.; Jones, A. A.; Kambour, R. P.; Bendler, J. T.; White, D. M. *Macromolecules* **1992**, *25*, 3031.
(4) Chung, G. C.; Kornfield, J. A.; Smith, S. D. *Macromolecules* **1994**, *27*, 964. Chung, G. C.; Kornfield, J. A.; Smith, S. D. *Macromolecules* **1994**, *27*, 5729.
(5) Arendt, B. H.; Kannan, R. M.; Zewail, M.; Kornfield, J. A.; Smith, S. D. *Rheol. Acta* **1994**, *33*, 322. Arendt, B. H.; Krishnamoorti, R.; Kornfield, J. A.; Smith, S. D. *Macromolecules* **1997**, *30*, 1127.
(6) Zawada, J. A.; Fuller, G. G.; Colby, R. H.; Fetters, L. J.; Roovers, J. *Macromolecules* **1994**, *27*, 6861.
(7) Miller, J. B.; McGrath, K. J.; Roland, C. M.; Trask, C. A.; Garroway, A. N. *Macromolecules* **1990**, *23*, 4543.
(8) Roovers, J.; Toporowski, P. M. *Macromolecules* **1992**, *25*, 1096. Roovers, J.; Toporowski, P. M. *Macromolecules* **1992**, *25*, 3454.
(9) Zawada, J. A.; Ylitalo, C. M.; Fuller, G. G.; Colby, R. H.; Long, T. E. *Macromolecules* **1992**, *25*, 2896.
(10) Colby, R. H. Int. Cong. Rheol., 10th **1988**, *1*, 278. Colby, R. H. *Polymer* **1989,** *30*, 1275.
(11) Zhao, Y.; Jasse, B.; Monnerie, L. *Polymer* **1989**, *30*, 1643.
(12) Composto, R. J.; Kramer, E. J.; White, D. M. *Polymer* **1990**, *31*, 2320.
(13) Alegria, A.; Colmenero, J.; Ngai, K. L.; Roland, C. M. *Macromolecules* **1994**, *27*, 4486.
(14) Le Menestrel, C.; Kenwright, A. M.; Sergot, P.; Lauprêtre, F.; Monnerie, L. *Macromolecules* **1992**, *25*, 3020.
(15) Cohen Addad, J. P.; Pellicioli, L.; Nusselder, J. J. H. *Polym. Gels Networks* **1997**, *5*, 201 and references cited therein.
(16) Cohen Addad, J. P. NMR and Fractal Properties of Polymeric Liquids and Gels. In *Progress in NMR Spectroscopy*; Emsley, J. W., Feeney, J., Sutcliffe, L. H., Eds.; Pergamon Press: Oxford, U.K., 1993.
(17) Sotta, P.; Fülber, C.; Demco, D. E.; Blümich, B.; Spiess, H. W. *Macromolecules* **1996**, *29*, 6222.

(18) Simon, G.; Baumann, K.; Gronski, W. *Macromolecules* **1992**, *25*, 3624.
(19) Lartigue, C.; Guillermo, A.; Cohen Addad, J. P. *J. Polym. Sci., B: Polym. Phys. Ed.* **1997**, *35*, 1095. Note that, in this reference, ϕ was used for the PEO weight fraction while, in the present paper, ϕ is used for the PEO volume fraction.
(20) Martuscelli, E.; Silvestre, C.; Addonizio, M. L.; Amelino, L. *Makromol. Chem.* **1986**, *187*, 1557.
(21) Ito, H.; Russell, T. P.; Wignall, G. D. *Macromolecules* **1987**, *20*, 2213.
(22) Hopkinson, I.; Kiff, F. T.; Richards, R. W.; King, S. M.; Farren, T. *Polymer* **1995**, *36*, 3523.
(23) Alfonso, G. C.; Russell, T. P. *Macromolecules* **1986**, *19*, 1143.
(24) Liberman, S. A.; Gomes, A. S.; Macchi, E. M. *J. Polym. Sci., Polym. Chem. Ed.* **1984**, *22*, 2809.
(25) Labouriau, A.; Cohen Addad, J. P. *J. Chem. Phys.* **1991**, *94*, 3242. Cohen Addad, J. P.; Labouriau, A. *J. Chem. Phys.* **1990**, *93*, 2911.
(26) Tsenoglou, C. *J. Polym. Sci., Part B: Polym. Phys. Ed.* **1988**, *26*, 2329.
(27) Cohen Addad, J. P.; Schmit, C. *Polymer* **1988**, *29*, 883.
(28) English, A. D. *Macromolecules* **1985**, *18*, 178 .
(29) Callaghan, P. T.; Samulski, E. T. *Macromolecules* **1997**, *30*, 113 .
(30) Marcinko, J. J.; Parker, A. A.; Shieh, Y. T.; Ritchey, W. M. *J. Appl. Polym. Sci.* **1992**, *45*, 391.
(31) Cohen Addad, J. P.; Guillermo, A. *J. Polym. Sci., Polym. Phys. Ed.* **1984**, *22*, 931.
(32) Brosseau, C.; Guillermo, A.; Cohen Addad, J. P. *Macromolecules* **1992**, *25*, 4535.
(33) Brereton, M. G. *Macromolecules* **1989**, *22*, 3667.
(34) Abragam, A. *The Principles of Nuclear Magnetism*; Oxford University Press: London, 1961.
(35) Wu, S. *J. Polym. Sci., Part B: Polym. Phys. Ed.* **1987**, *25*, 2511.

MA970836V